

# A review on the effect of welding on the corrosion of magnesium alloys

**N S Mohamed and J Alias\***

Structural Materials and Degradation, Faculty of Mechanical Engineering, Universiti Malaysia Pahang (UMP), 26600 Pekan, Pahang.

Corresponding Author: juliawati@ump.edu.my

**Abstract.** Welding is an important joining technique for lightweight alloys with their increasing applications in aerospace, aircraft, automotive, electronics and other industries. The applications of lightweight alloys particularly magnesium alloys increased rapidly due to their beneficial properties such as low density, high strength-to-mass ratio, good dimensional stability, electromagnetic shielding and good recyclability. The effect of welding on the corrosion of magnesium alloys are reviewed in this paper, which closely related to the developed microstructure by the welding process. The paper focuses particularly on friction stir and laser welding. The basic principles of friction stir and laser welding are discussed, to present the likelihood of defects which significantly affect the corrosion of magnesium alloy. The finding in corrosion demonstrated the morphology of corrosion occurrence on each welded region, and observation on the potential and current values are also included.

## 1. Introduction

Magnesium is extremely light metal with excellent specific strength [1], excellent sound damping capabilities [2], good cast-ability [3], hot formability [4], excellent machinability, good electromagnetic interference shielding and recyclability [5]. However, their poor resistance to corrosion and wear, limits their wider applications [6]. Mg is generally an active metal and its corrosion behavior is significantly influenced by the microstructure [6].

The alloying elements are normally added to increase the strength. This consequently led to the formation of large intermetallic precipitates during casting. These precipitates are too large to be greatly affected by sub-sequent thermo mechanical processing. However the presence of these precipitates in the microstructure could reduce the material resistance to corrosion [7].

Work by Cao [5] shows magnesium alloy components can be joined using mechanical fasteners as well as a variety of welding methods including tungsten-arc inert gas (TIG), metal-arc inert gas (MIG), plasma arc, electron, laser, friction, adhesive, explosion, stud, ultrasonic, and spot welding. TIG and MIG processes are the main common welding method methods for magnesium alloys. However, low welding speeds, large heat affected zone (HAZ) and fusion zone (FZ), high shrinkages, variations in microstructures and properties, evaporative loss of alloying elements, high residual stress and distortion of



arc-welded joints have caused attention to be drawn towards laser welding [1, 5]. Besides laser welding, friction stir welding (FSW) is capable of joining magnesium alloys without melting and thus it can eliminate problems related to the solidification [2]. As FSW does not require any filler material, the metallurgical problems associated with it can also be eliminated and good quality weld can be obtained.

## 2. Welding process

Friction stir weld (FSW) is solid state material joining process that was invented in 1991 at The Welding Institute (TWI) of the United Kingdom [8]. It was initially applied to aluminum alloys and resulting large strain of material at high temperature without melting the base material [9]. The mechanism of friction stir welding working is by applying a non-consumable rotating tool with a particularly designed pin and shoulder that are inserted into the abutting edges of the joining plates. The tools then subsequently pass through the joint line definition of the tool and work piece as shown in Figure 1 [3].

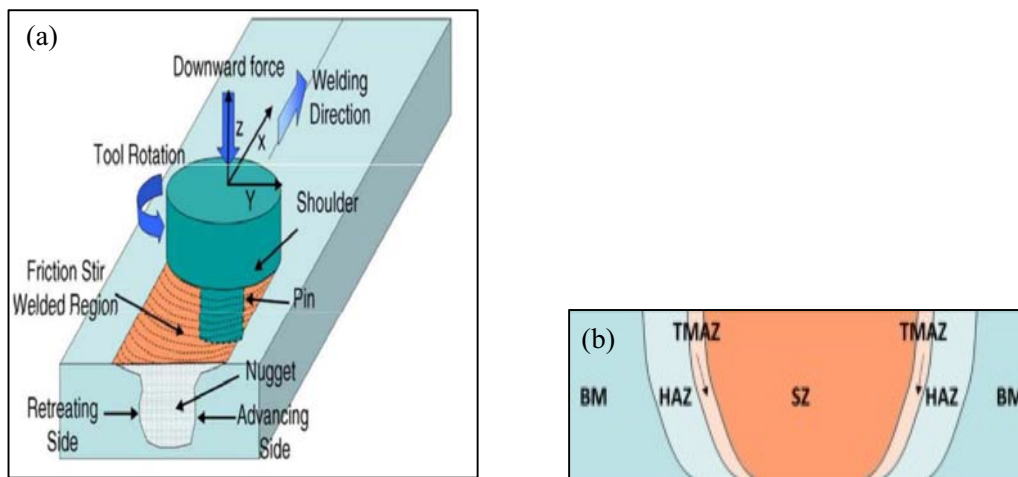


**Figure 1.** (a) Frictions stir welding process [8], (b) a typical micrograph showing various microstructural zones in FSW, stir zone (SZ), thermomechanical heat affected zone (TMAZ), heat affected zone (HAZ) and base metal (BM) [10].

**Table 1.** FSW parameters for mechanized welding [8].

No.	Parameter	Effect of parameter
a	Rotational speed	Frictional heat, stirring, oxide layer breaking and mixing of material
b	Welding speed	Appearance, heat control
c	Pressure on tool (down force)	Frictional heat, maintaining contact conditions
d	Tilting angle	Appearance of weld, thinning

The tool produces the thermo mechanical deformation and work piece frictional heating necessary for friction stirring. When the down force is applied on tool then tool is inserting in the base materials. The friction stirring tool consists of a pin or probe, and shoulder. Contact of the pin with the work piece creates frictional and deformational heating and softens the work piece material contacting the shoulder to the work piece increases the work piece heating, expands the zone of softened material, and constrains the

deformed material [3, 8] The correct tool material determines material characteristics that are important for each friction stir application including wear resistance, coefficient of thermal expansion, elevated temperature strength, tool reactivity, fracture toughness, machinability and microstructure uniformity [8].

The shape of the tool pin (or probe) influences the flow of plasticized material and affects weld properties. Optimizing tool geometry to produce more heat or achieve more efficient “stirring” offers improvement in breaking and mixing of the oxide layer and more efficient heat generation, yielding higher welding speeds and, enhanced weld quality [8].

Most complex motion tools require specialized machinery or specially machined tools, making these tools unsuitable for basic applications [11].

**Table 2.** Complex motion tool [8, 11].

No.	Type of tools	Description of the type of tools
a	Skew-stir Tool	Increase the volume of material swept by pin to pin volume ratio by offsetting the axis of the pin from the axis of spindle
b	Com-stir Tool	Combine rotary motion (tool shoulder) with orbital motion (tool pin) to maximize the volume of material swept by pin to pin volume ratio
c	Dual-rotation Tool	The pin and shoulder rotate separately at different speeds and/or in different directions
d	Re-stir tool	Avoid the inherent asymmetry produced during friction stirring by alternating the tool rotation, either by angular reciprocation (direction reversal during one revolution) or rotary reversal (direction reversal every one or more revolutions) Alternating the tool rotation produces alternating regions of advancing and retreating side material through the length of the weld, thus eliminating the asymmetry issues

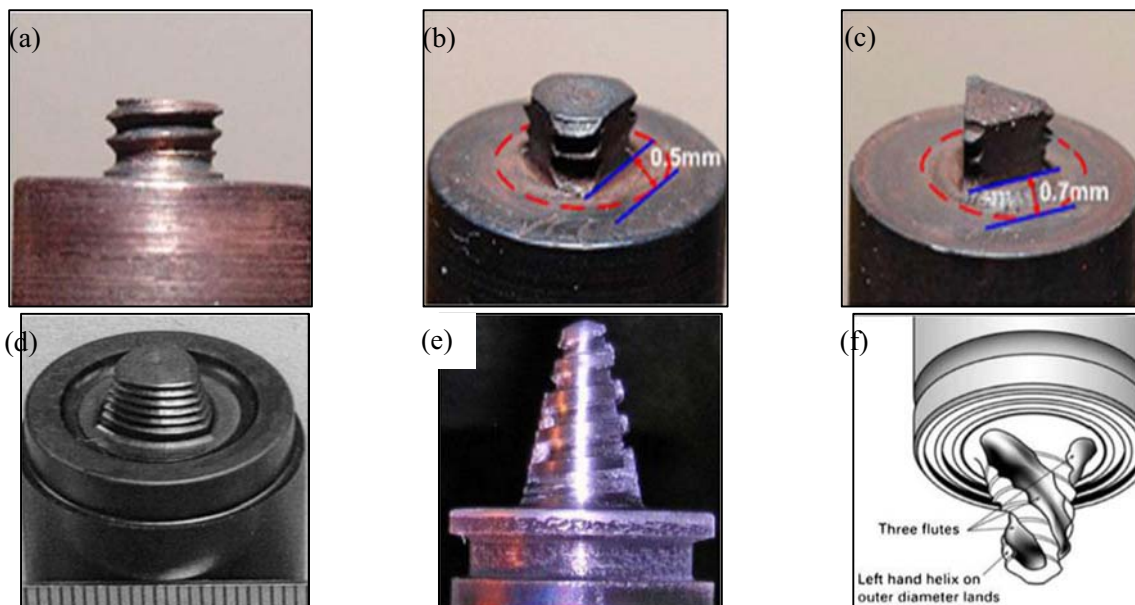


**Figure 2.** Commonly used pin geometries (a) cylinder threaded, (b) three flat threaded, (c) triangular, (d) trivex, (e) threaded conical, and (f) schematic of a triflute [8].

### 3. Laser welding

The effectiveness of laser welding depends on the physical properties of the material to be welded. Cao [5] state that magnesium alloys possess certain natural characteristics such as low absorptivity of laser beams, strong tendency to oxidize, high thermal conductivity, high coefficient of thermal expansion, low melting and boiling temperatures, wide solidification temperature range, high solidification shrinkage, a tendency to form low melting-point constituents, low viscosity, low surface tensions, high solubility for hydrogen in the liquid state, and absence of color change at the melting point temperature [1, 5, 12]. Therefore during laser welding of magnesium alloys, some processing problems and weld defects can be encountered. The following discussion focuses on some important processing variables and their influence on the weld quality of magnesium alloy.

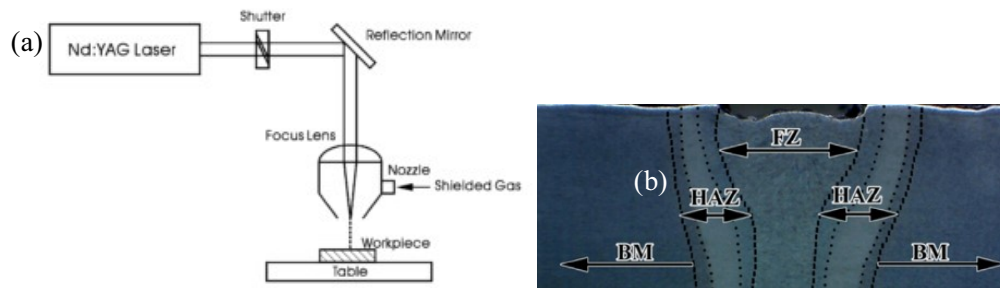


**Figure 3.** (a) The Nd:YAG laser welding system [1] (b) a typical micrograph showing various microstructural zones in laser welding, fusion zone (FZ), heat affected zone (HAZ) and base metal (BM) [13].

#### 3.1. Laser power

High power density at the work piece is crucial to achieve keyhole welding and to control the formation of welds. Figure 4 shows the effect of laser power on the penetration depth (Figure 4(a)) and weld width (Figure 4(b)) for WE43 alloy welded at a speed of 33 mm/s and a focused diameter of 0.25mm [5, 14]. High beam powers led to deep and wide beads, and reduce both ripples and crowning [5]. Lehner [15] reported that a lower power level and a slower speed lead to better weld quality.

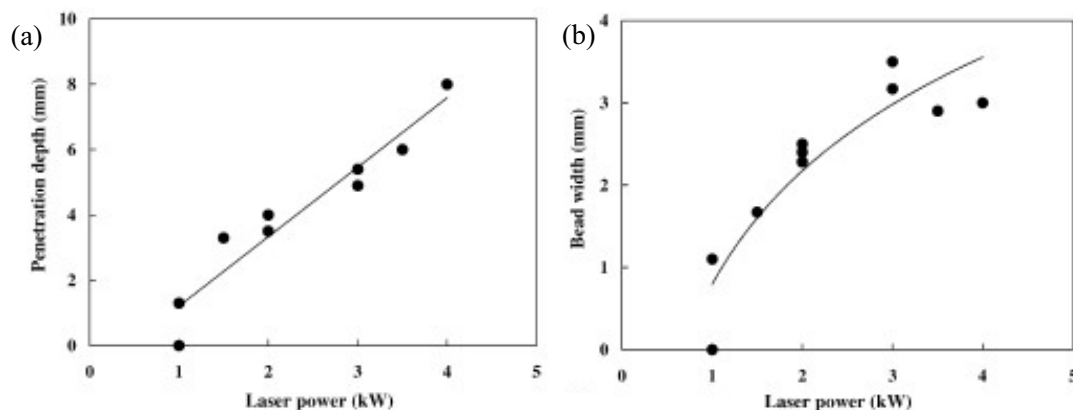


**Figure 4.** Effect of CO<sub>2</sub> laser power on (a) penetration depth (b) bead width of cast WE43 alloy joints [5].

### 3.2. Welding speed

Figures 5 and 6 show the effects of welding speed on penetration depth and weld width at different levels of power for CO<sub>2</sub> and Nd:YAG lasers, respectively. The penetration depth and weld width both decrease linearly with increasing welding speed.

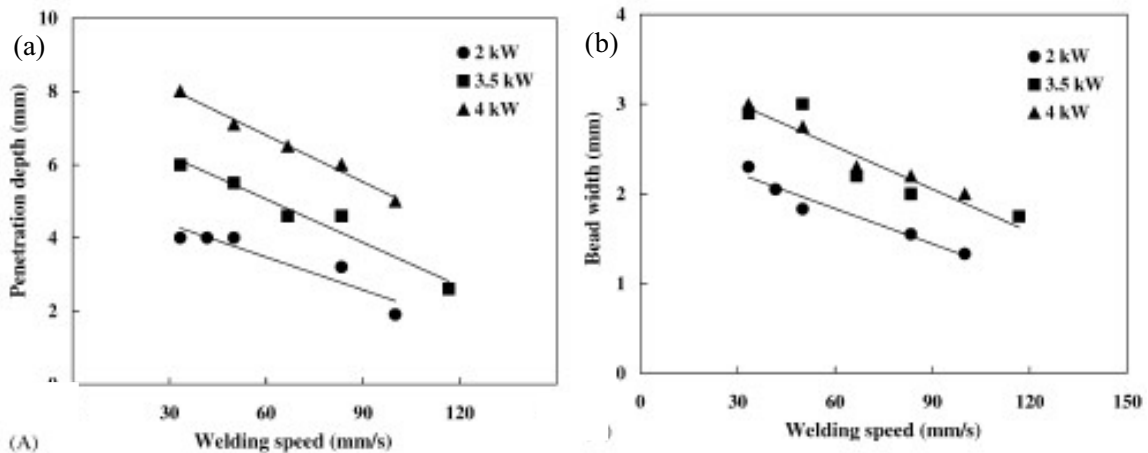


**Figure 5.** Effect of welding speed on (a) penetration depth, and (b) bead width of cast WE43 alloy joints welded using CO<sub>2</sub> laser [5], [14].

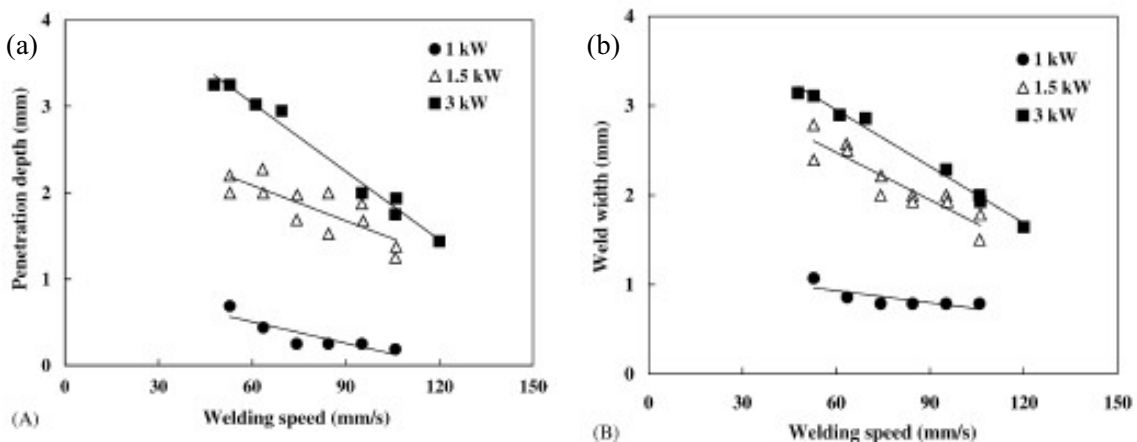


**Figure 6.** Effect of welding speed on (a) penetration depth, and (b) weld width for die-cast AM60B alloy joints welded using a ND:YAG [5], [16].

Too high welding speed was reported to reduce ripples but greatly increase crowning, or even to increase tendency to brittleness in the fusion zone [5]. Clearly the welding speed should be adjusted to provide the penetration depth required at a given power level. The research into laser welding processes for magnesium alloys is still in its infancy. Much more work, therefore, is needed to systematically investigate the laser welding characteristics of different magnesium alloys because of the difference in their thermal properties.

#### 4. Corrosion of welded magnesium alloy

The corrosion behavior of magnesium alloy is depending on variety factor such as pH value [17], and if the pH value is above 12, a stable and self-healing passive layer developed, and is responsible for high corrosion resistance [18]. It is confirmed that the friction stir welded metal could enhance the corrosion rate with a decrease in pH value, remain constant in neutral pH value and a comparatively very low corrosion rate in alkaline solution.

Figure 7 shows the corrosion and pit morphology of the welded magnesium alloy after immersion tests at pH 3, 7 and 11 with constant chloride ion concentration of 0.60 mol/L. It is found that at a lower concentration of chloride ion the surface of the welded alloy was slightly corroded in neutral solution while it was severely corroded at a higher concentration of chloride ion [18]. From the morphology of welded metal after immersion test, it is observed that the base metal shows the pitting marks and pitting corrosion take place at the welded microstructure [19]. The number of pits are highly seen in the welded metal region when it is immersed in the solution of low pH [20]. Moreover, the increase of grain boundary in the weld metal region acts cathode causing micro-galvanic effect [17]. Corrosion tends to be concentrated in the area adjacent to the grain boundary until the grain may be undercut and fall out [18].

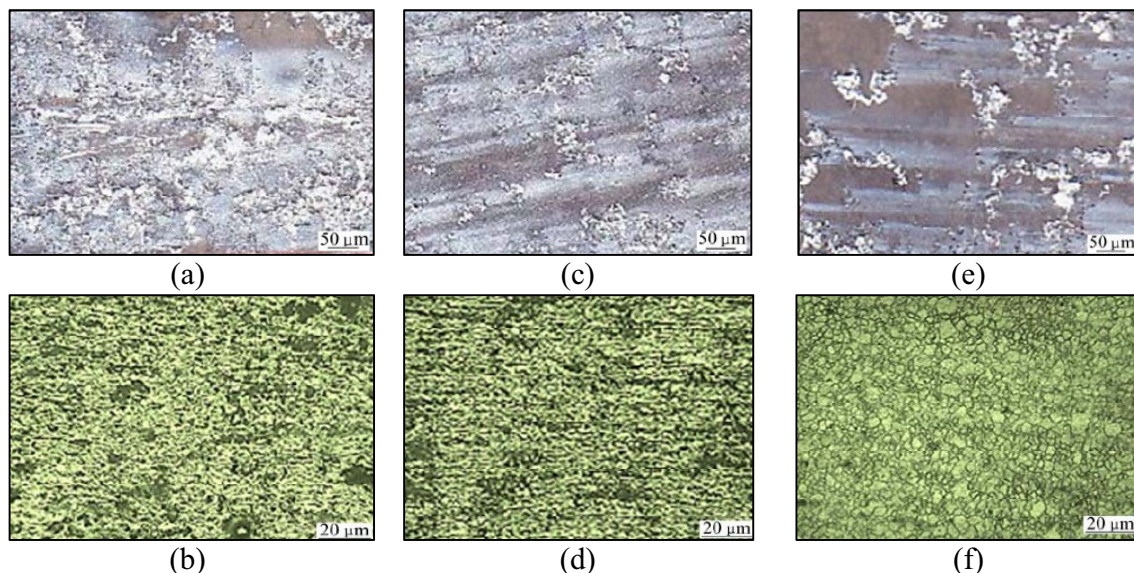


**Figure 7.** Effect of pH on corrosion morphology (a), (c), (e) and pit morphology (b), (d), (f), pH=3; (a), (b) pH=7; (c), (d) pH=11; (e), (f) [18].

A study by Ghali [21] examined that corrosion potential of Mg is slightly negative than -1.5 V in dilute chloride solution with respect to the standard electrode potential at 25°C is -2.37 V. Recent study by Argade [22] revealed that the corrosion properties of a welded Mg-Y-RE alloy in four different conditions, (i) A: as-received, (ii) B: as-received samples subjected to peak age hardening treatment of 210°C for 48 h, (iii) C: friction stir weld (FSW) of B-type material, and (iv) D: FSW of A-type material subjected to subsequent peak age hardening treatment of 210°C for 48 h. The potentiodynamic polarization plots for all four conditions of Mg-Y-RE alloy in 3.5 wt.% NaCl solution are shown in Figure 8.

For type-A and type-B, the anodic branch showed a linear region in the potential range of -1800 to -1700 mV vs. SCE as can be seen in Figure 8. In case of type-C and type-D a small linear region in the

anodic branch was observed as compared to type-A and type-B. Among all the microstructural conditions, type-D showed the highest positive value of  $E_{\text{corr}}$  and the lowest value of  $i_{\text{corr}}$ . The comparative  $E_{\text{corr}}$  and  $i_{\text{corr}}$  values of different conditions were observed in the following order: (a)  $E_{\text{corr}}$ : type-D > type-C > type-B > type-A, and (b)  $i_{\text{corr}}$ : type-D < type-B < type-A < type-C. The details of the polarization parameter are summarized in Table 3. The SEM micrographs (Figures 9(a) and (b)) indicated the localized corrosion attack for type D material with deeper pit attack in comparison to the type B material.

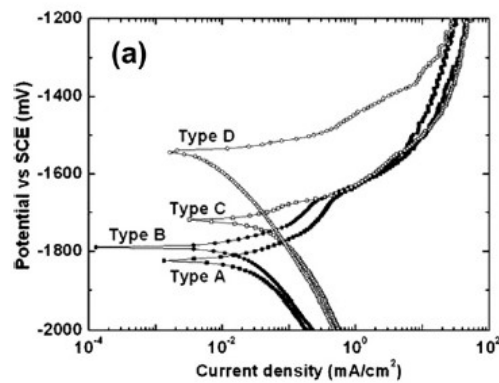


**Figure 8.** Polarization plots of Mg-Y-RE alloy conditions [22].

**Table 3.** Electrochemical parameters from LPP for Mg-Y-RE alloy conditions [22].

Sample Conditions	Corrosion Potential $E_{\text{corr}}$ (mV vs. SCE)	Current Density $i_{\text{corr}}$ (A/cm <sup>2</sup> )
Type A	$-1823 \pm 22$	$5.9 \pm 0.4 \times 10^{-5}$
Type B	$-1788 \pm 15$	$2.7 \pm 0.2 \times 10^{-5}$
Type C	$-1719 \pm 25$	$8.7 \pm 0.4 \times 10^{-5}$
Type D	$-1544 \pm 28$	$1.3 \pm 0.1 \times 10^{-5}$

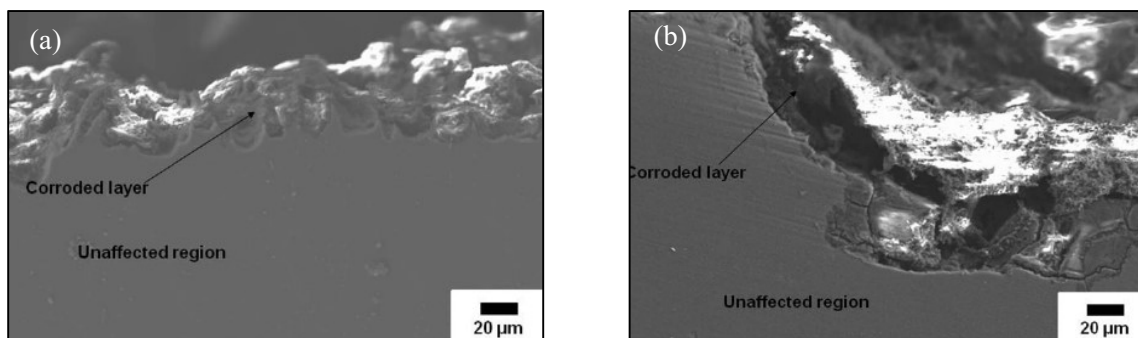


**Figure 9.** SEM micrographs of cross-section of LPP tested (a) type B material and (b) type D material [23].

## 5. Conclusions

The friction stir and laser welding of magnesium alloys have been reviewed. The welding parameters such as welding speed, tool material and shape, tilting angle could affect the welding quality and induces microstructure variation and surface character of welded magnesium alloy. It is consequently affect the pit attack morphology and corrosion behavior, as observed from the potentiodynamic polarization plot and cross-section images.

## References

- [1] L. Kwang, C. Chung, Y. Ching, and K. Chyn, "Optimization of Nd : YAG laser welding onto magnesium alloy via Taguchi analysis," vol. 37, pp. 33–42, 2004.
- [2] S. Mironov, T. Onuma, Y. S. Sato, and H. Kokawa, "Microstructure evolution during friction-stir welding of AZ31 magnesium alloy," *Acta Mater.*, vol. 100, pp. 301–312, 2015.
- [3] R. S. Mishra and Z. Y. Ma, "Friction stir welding and processing," *Mater. Sci. Eng. R Reports*, vol. 50, no. 1–2, pp. 1–78, 2005.
- [4] G. L. Song and Z. Xu, "The surface, microstructure and corrosion of magnesium alloy AZ31 sheet," *Electrochim. Acta*, vol. 55, no. 13, pp. 4148–4161, 2010.
- [5] X. Cao, M. Jahazi, J. P. Immarrigeon, and W. Wallace, "A review of laser welding techniques for magnesium alloys," *J. Mater. Process. Technol.*, vol. 171, no. 2, pp. 188–204, 2006.
- [6] B. A. James, "Localized Corrosion of Friction Stir Spot Welds in Magnesium AZ31 Alloy Localized Corrosion of Friction Stir Spot Welds," 2012.
- [7] N. N. Aung and W. Zhou, "Effect of grain size and twins on corrosion behaviour of AZ31B magnesium alloy," *Corros. Sci.*, vol. 52, no. 2, pp. 589–594, 2010.
- [8] K. R. Pagar and P. A. D. Wable, "Review Paper : Friction Stir Welding ( FSW )," vol. 6, no. 5, pp. 123–129, 2016.
- [9] R. C. Zeng, J. Chen, W. Dietzel, R. Zettler, J. F. dos Santos, M. Lucia Nascimento, and K. U. Kainer, "Corrosion of friction stir welded magnesium alloy AM50," *Corros. Sci.*, vol. 51, no. 8, pp. 1738–1746, 2009.
- [10] R. Sharma and O. P. Singh, "Effect of FSW Process Parameters on Mechanical Properties of Polypropylene : An Experimental Study," vol. 2, no. 12, pp. 7792–7798, 2013.
- [11] R. Rai, A. De, H. K. D. H. Bhadeshia, and T. DebRoy, "Review: friction stir welding tools," *Sci. Technol. Weld. Join.*, vol. 16, no. 4, pp. 325–342, 2011.
- [12] C. Taltavull, B. Torres, A. J. Lopez, P. Rodrigo, E. Otero, A. Atrens, and J. Rams, "Corrosion behaviour of laser surface melted magnesium alloy AZ91D," *Mater. Des.*, vol. 57, pp. 40–50, 2014.
- [13] X. N. Wang, C. J. Chen, H. S. Wang, S. H. Zhang, M. Zhang, and X. Luo, "Microstructure formation and precipitation in laser welding of microalloyed C-Mn steel," *J. Mater. Process. Technol.*, vol. 226, pp. 106–114, 2015.
- [14] S. Ignat, P. Sallamand, D. Grevey, and M. Lambertin, "Magnesium alloys (WE43 and ZE41) characterisation for laser applications," *Appl. Surf. Sci.*, vol. 233, no. 1–4, pp. 382–391, 2004.
- [15] C. Lehner, G. Reinhart, and L. Schaller, "Welding of die-casted magnesium alloys for production," *J. Laser Appl.*, vol. 11, no. 5, p. 206, 1999.
- [16] E. Aghion and B. Bronfin, "Magnesium Alloys Development towards the 21<sup>st</sup> Century," *Mater. Sci. Forum*, vol. 350–351, pp. 19–30, 2000.
- [17] S. Bender, J. Goellner, A. Heyn, and E. Boese, "Corrosion and corrosion testing of magnesium alloys," *Mater. Corros.*, vol. 58, no. 12, pp. 977–982, 2007.
- [18] A. Dhanapal, S. Rajendra Boopathy, and V. Balasubramanian, "Corrosion behaviour of friction stir welded AZ61A magnesium alloy welds immersed in NaCl solutions," *Trans. Nonferrous Met. Soc. China (English Ed.)*, vol. 22, no. 4, pp. 793–802, 2012.

- [19] J. Verma and R. V. Taiwade, “Effect of welding processes and conditions on the microstructure , mechanical properties and corrosion resistance of duplex stainless steel weldments — A review,” vol. 25, pp. 134–152, 2017.
- [20] W. Yuan, R. S. Mishra, B. Carlson, R. Verma, and R. K. Mishra, “Material flow and microstructural evolution during friction stir spot welding of AZ31 magnesium alloy,” *Mater. Sci. Eng. A*, vol. 543, pp. 200–209, 2012.
- [21] E. Ghali, W. Dietzel, and K. U. Kainer, “General and localized corrosion of magnesium alloys: A critical review,” *J. Mater. Eng. Perform.*, vol. 22, no. 10, pp. 2875–2891, 2013.
- [22] G. R. Argade, K. Kandasamy, S. K. Panigrahi, and R. S. Mishra, “Corrosion behavior of a friction stir processed rare-earth added magnesium alloy,” *Corros. Sci.*, vol. 58, pp. 321–326, 2012.
- [23] F. Gharavi, K. A. Matori, R. Yunus, N. K. Othman, and F. Fadaeifard, “Corrosion behavior of Al6061 alloy weldment produced by friction stir welding process,” *J. Mater. Res. Technol.*, vol. 4, no. 3, pp. 314–322, 2015.